The Astrophysical Journal Letters, 889:L22 (8pp), 2020 January 20 https://doi.org/10.3847/2041-8213/ab6560
© 2020. The American Astronomical Society. All rights reserved.

Physics of Prodigious Lyman Continuum Leakers

Renyue Cen
Princeton University Observatory, Princeton, NJ 08544, USA; cen@astro.princeton.edu
Received 2019 September 30; revised 2019 December 13; accepted 2019 December 23; published 2020 January 24

Abstract

An analysis of the dynamics of a star formation event is performed. It is shown that galaxies able to drive leftover gas to sufficient altitudes in a few million years are characterized by two basic properties: small sizes ($\leqslant$1 kpc) and high star formation rate (SFR) surface densities ($\Sigma_{\rm SFR} \geqslant 10\,M_\odot\,{\rm yr}^{-1}\,{\rm kpc}^{-2}$). For the parameter space of relevance, the outflow is primarily driven by supernovae with radiation pressure being significant but subdominant. Our analysis provides the unifying physical origin for a diverse set of observed Lyman continuum photons (LyC) leakers, including the green-pea galaxies, [S II]-weak galaxies, and Lyα emitters, with these two characteristics as the common denominator. Among verifiable physical properties of LyC leakers, we predict that (1) the newly formed stellar masses are typically in the range of 10^8–$10^{10}\,M_\odot$, except perhaps ultra-luminous infrared galaxies (ULIRGs), (2) the outflow velocities are typically in the range typically of 100–600 km s^{-1}, but may exceed 10^3 km s^{-1} in ULIRGs, with a strong positive correlation between the stellar masses formed and the outflow velocities, (3) the overall escape fraction of galaxies is expected to increase with increasing redshift, given the cosmological trend that galaxies become denser and more compact with increasing redshift. In addition, two interesting by-product predictions are also borne out. First, ULIRGs appear to be in a parameter region where they should be prodigious LyC leakers, unless there is a large ram pressure due to infalling gas with a rate exceeding about 30 times the SFR. Then, toward the tail end of a ULIRG event when the ram pressure relents, advanced ULIRGs are expected to leak more LyC photons than earlier ULIRGs. Second, Lyman-break galaxies (LBGs) are not supposed to be prodigious LyC leakers in our model, given their claimed effective radii exceeding 1 kpc. Thus, if LBGs are observed to have LyC leakers, it may be that the effective radii of their star-forming regions have been overestimated by a factor of 2–4.

Unified Astronomy Thesaurus concepts: Starburst galaxies (1570); Compact galaxies (285); Ultraluminous infrared galaxies (1735); Lyman-break galaxies (979); Reionization (1383); Emission line galaxies (459); Supernovae (1668); Star formation (1569); Milky Way Galaxy (1054); Star forming regions (1565)

1. Introduction

Understanding how Lyman continuum photons (LyC) escape from galaxies is necessary for understanding the epoch of reionization (EoR), one of the last major frontiers of astrophysics. High-resolution cosmological hydrodynamic galaxy formation simulations have widely evidenced that supernova-feedback-driven blastwaves are the primary facilitator to evacuate or create major pores in the interstellar medium (ISM) to enable the escape of LyC (e.g., Wise & Cen 2009; Kimm & Cen 2014; Cen & Kimm 2015; Ma et al. 2016; Kimm et al. 2019). Because LyC escape is not directly measurable at EoR due to its limited mean free path, it is imperative to ascertain this unknown by establishing observable proxies for the escape fraction, $f_{\rm esc}$, when both proxies and $f_{\rm esc}$ are measurable at lower redshift, based upon a satisfactory physical understanding.

Observationally, in the low-z ($z < 0.4$) universe the majority of galaxies with large $f_{\rm esc}$ values turn out to belong to the compact, so-called green-pea galaxies from the Sloan Digital Sky Survey (SDSS) sample, characterized by their low stellar masses, low metallicities, very strong nebular emission lines (Hβ equivalent widths $>$200 Å) and very high flux ratios of [O III]5007/[O II]3727 > 5 (e.g., Izotov et al. 2016a, 2016b, 2018a, 2018b, 2019; Schaerer et al. 2016). Interestingly, the green-pea galaxies have star formation rate (SFR) surface densities of 10–100 $M_\odot\,{\rm yr}^{-1}\,{\rm kpc}^{-2}$, which are much higher than typical star-forming galaxies in the local universe but may be similar to those at EoR. Another class of low-redshift galaxies that have high LyC escape fraction is identified by their high Lyα emission (e.g., Verhamme et al. 2015, 2017), which typically have SFR surface densities of $\sim$10 $M_\odot\,{\rm yr}^{-1}\,{\rm kpc}^{-2}$). At $z \sim 3$ LyC escape is detected in dozens of individual galaxies (e.g., Mostardi et al. 2015; Shapley et al. 2016; Vanzella et al. 2016; Steidel et al. 2018), some of which also show intense [O III] emission that are consistent with low-z observations and characteristic of galaxies at EoR (e.g., Fletcher et al. 2019). Furthermore, recently another set of galaxies with relatively weak [S II] nebular emission lines are also observed to show high LyC escape (Wang et al. 2019). The low-redshift green-pea galaxies, $z \sim 3$ high LyC leakers and the [S II]-weak LyC leaking galaxies are different in various respects, such as stellar mass, metallicity, dust content, and ISM properties. But all appear to share two common characteristics: all four have very high SFR surface densities and relatively compact sizes.

This Letter aims to understand if supernova feedback may be the common physical process that underwrites the commonality shared by these different classes of galaxies observed. We will show that this is indeed the case. This finding thus provides a physical basis to help identify galaxies with high LyC leakage at the EoR by indirect but robust markers that can be established at more accessible redshift, and for why dwarf galaxies at EoR are much more capable of enabling high LyC escape fraction than typical low-redshift counterparts.

2. Physics of Lyman Continuum Leakers

We explore if gas density-bound structures in star-forming galaxies may be produced. The following treatment is undoubtedly simplified but captures the essence of the physics, and is primarily a means to identify likely physical parameter space that is relevant for making galaxies with high LyC escape fractions. A gas cloud of initial mass $M_{\rm gas,0}$ with a half-light radius r_h and an SFR gives rise to an outward radial force on the gas cloud itself due to supernova explosion generated radial momentum equal to

$$F_{\rm SN} = {\rm SFR} \times p_{\rm SN} \times M_{\rm SN}^{-1}, \quad (1)$$

where $p_{\rm SN} = 3 \times 10^5\, M_\odot$ km s^{-1} is the terminal momentum generated per supernova (e.g., Kimm & Cen 2014), $M_{\rm SN}$ is the amount of stellar mass formed to produce one supernova, which is equal to about (50, 75, 100) $M_\odot$ for (Chabrier, Kroupa, Salpeter) initial mass function (IMF), respectively. The exact value of $p_{\rm SN}$ weakly depends on density and metallicity of the ambient gas. For simplicity without loss of validity given the concerned precision of our treatment, we use the above fiducial value. Another mechanical form of feedback from massive stars is fast stellar winds due to O stars. The total energy from stellar winds is about a factor of 10 lower than the total energy from supernovae (e.g., Leitherer et al. 1999). Because stellar winds roughly track core-collapse supernovae, we simply omit stellar winds bearing a loss of accuracy at 10% level. The second important outward force on the gas is the radiation pressure on dust grains, equal to

$$F_{\rm rad} = {\rm SFR} \times \alpha \times c[1 - \exp(-\Sigma_{\rm gas}\kappa_{\rm UV})] \times (1 + \Sigma_{\rm gas}\kappa_{\rm FIR}), \quad (2)$$

where $\alpha = 3.6 \times 10^{-4}$ is an adopted nuclear synthesis energy conversion efficiency from rest mass to radiation, c speed of light, $\kappa_{\rm UV} = 1800$ cm^2 g^{-1} and $\kappa_{\rm FIR} = 20$ cm^2 g^{-1} the opacity at ultraviolet (UV; e.g., Draine 2003) and dust processed radiation far-infrared (FIR) radiation (e.g., Lenz et al. 2017), respectively, $\Sigma_{\rm gas}$ the surface density of the gas. The exact value of $\kappa_{\rm UV}$ matters little in the regime of interest but variations of the value of $\kappa_{\rm FIR}$ does matter to some extent. To place the two forces in relative terms, we note that at $\Sigma_{\rm gas} = 1.3 \times 10^4\, M_\odot$ pc^{-2}, the radiation pressure due to infrared (IR) photons equals the ram pressure due to supernova blastwaves, with the former and latter dominating at the higher and lower surface densities, respectively.

There are two relevant inward forces. The mean gravitational force, when averaged over an isothermal sphere, which is assumed, is

$$F_g = \frac{\ln(r_{\rm max}/r_{\rm min}) G M_{\rm gas,0} M_{\rm gas}(t)}{4 r_h^2}, \quad (3)$$

where $r_{\rm min}$ to $r_{\rm max}$ are minimum and maximum radii of the gas cloud being expelled. For our calculations below we adopt $r_{\rm min} = 100$ pc and $r_{\rm max} = r_h$; the results depend weakly on the particular choices of these two radii. We note that $M_{\rm gas}(t)$ is the remaining mass of the gas cloud when it starts to be lifted at time t_L by the combined force of supernova-driven momentum flux and radiation-momentum flux against inward forces, with $M_{\rm gas,0} - M_{\rm gas}(t_L)$ having formed into stars. Another inward force is that due to ram pressure, which we parameterize in terms of gas infall rate in units of SFR:

$$F_{\rm rp} = \dot{M}_{\rm inf} v_{\rm inf} = \eta \times {\rm SFR} \times \left(\frac{G M_{\rm gas,0}}{r_h}\right)^{1/2}, \quad (4)$$

where η is the ratio of mass infall rate to SFR.

The relevant physical regime in hand is how to drive the gas by the combined force of supernovae and radiation against the combined force of gravitational force and ram pressure. A key physical requirement, we propose, is that the feedback process needs to promptly lift the entire remaining gas cloud to a sufficient height such that it piles itself into a (thin) shell that subsequently fragments while continuing moving out, in order to make a copious LyC leaker. It seems appropriate to define "a sufficient height" as a height on the order of r_h, which we simplify to be just r_h. The above definition may be expressed as

$$(F_{\rm SN} + F_{\rm rad} - F_g - F_{\rm rp})(t_h - t_L) = M_{\rm gas}(t_L) v_h \quad \text{and} \quad 2 r_h = (t_h - t_L) v_h, \quad (5)$$

where v_h is the shell velocity when reaching r_h at time t_h, and $M_{\rm gas}(t_L)$ is the gas cloud mass at t_L when it begins its ascent.

We may relate the initial gas mass $M_{\rm gas,0}$ to SFR that is observable by using an empirically found relation:

$${\rm SFR} = c_* M_{\rm gas,0}/t_{\rm dyn}, \quad (6)$$

where G is the gravitational constant, $t_{\rm dyn} = \sqrt{\frac{3\pi}{32 G \rho_t}}$ is the dynamical time of the system with ρ_t being the total density, the sum of gas and stars within r_h, star formation efficiency per dynamical time is found to be $c_* = 0.01$ (Krumholz et al. 2012). Note that the SFR above is the SFR up to the time t_L, when it is shut down upon the uplift of the gas cloud.

We compute the rate of supernova explosion more precisely. This is needed because as soon as the combined outward force of supernova feedback and radiation pressure is stronger than inward forces at time t_L, we need to stop star formation then. It is possible in some cases that the star formation has not lasted long enough to reach the saturation supernova rate. We use a recent, comprehensive analysis of Zapartas et al. (2017) that takes into account both single and binary stellar populations, including supernovae due to binary mergers. We convolve the fitting formula (A.2) in Zapartas et al. (2017) that is composed of three separate temporal segments, 3–25 and 25–48 Myr due to massive single stars and 448–200 Myr due to binary merger produced core-collapse supernovae, with a constant SFR (Equation (6)) starting at time $t = 0$. Figure 1 shows the resulting instantaneous supernova rate as a function of time for a star formation event at a constant SFR $= 1\ M_\odot$ yr^{-1}. Then, $M_{\rm SN}(t) = 1\ M_\odot/N_{\rm ccSN}$ (where $N_{\rm ccSN}$ is the y-axis shown in Figure 1) as a function of time since the start of the starburst, in lieu of a constant value of $M_{\rm SN}$ that is the saturation value at $t \geqslant 200$ Myr, in Equation (1), where appropriate. We note that at $t \geqslant 200$ Myr the saturation rate corresponds to one supernova per 78 $M_\odot$ of stars formed, approximately corresponding to a Kroupa IMF.

Figure 2 shows the results by integrating Equation (5). The solid red contours labeled in units of Myr shows the time, $t_h - t_L$, which it takes to drive the gas to an altitude of r_h. Earlier we mentioned the need of "promptly" driving the gas away, which we now elaborate. For any starburst event, massive O stars formed that dominate the LyC radiation die in

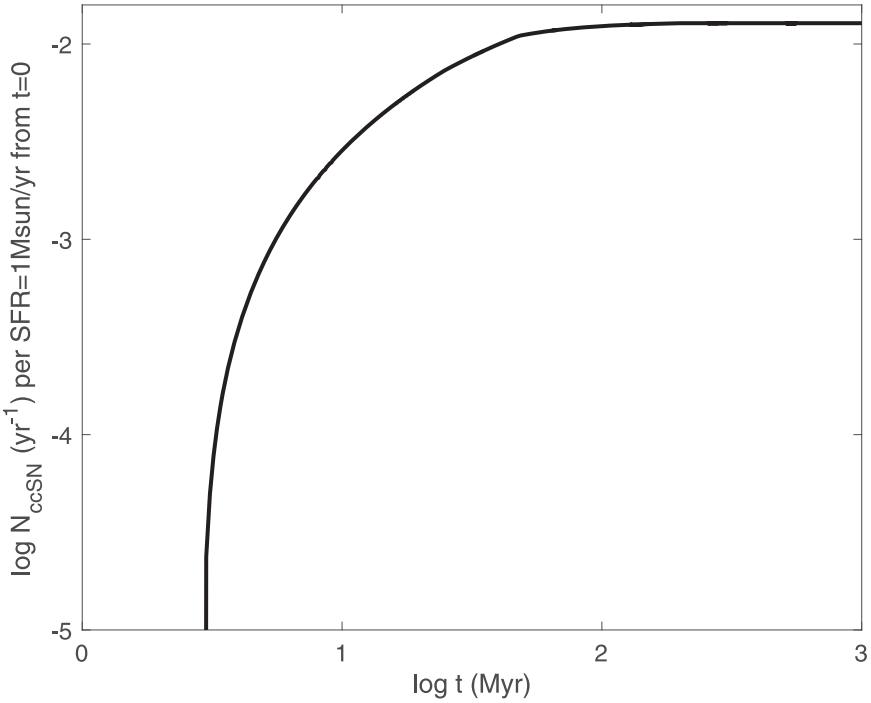

Figure 1. Supernova rate for a star formation event at an SFR of 1 $M_\odot$ yr^{-1} starting at time $t = 0$ as a function of time. This plot is produced using Equation (A.2) of Zapartas et al. (2017) of the core-collapse supernova rate including both single stars and binary mergers. We note that at $t \geqslant 200$ Myr the saturation rate corresponds to one supernova per 78 $M_\odot$ of stars formed, approximately in agreement with what a Kroupa IMF gives.

about 5 Myr. Therefore, the time elapsed since the end of the starburst of the observed prodigious LyC leakers should not be longer than that timescale, i.e., $t_h - t_L \leqslant 5$ Myr. Comparing the $t_h - t_L = 5$ Myr contour with the black solid triangles indicates that all the observed LyC leakers lie in the parameter region with $t_h - t_L \leqslant 5$ Myr, except J0921 with $r_h = 0.78$ kpc, SFR $= 7.68$ $M_\odot$ yr^{-1} and $M_* = 6.3 \times 10^{10}\, M_\odot$ and J0926 with $r_h = 0.69$ kpc, SFR $= 3.47$ $M_\odot$ yr^{-1} and $M_* = 1.3 \times 10^9\, M_\odot$ (Alexandroff et al. 2015). In the entire region of possible prodigious LyC leakers we point out that the outward force is dominated by supernova-driven momentum, although in a thin top-left wedge region the radiation pressure alone is also able to counter the gravity. It is very clear that all LyC leakers live in a parameter space generally denoted as Lyα emitters, as indicated by the large, cyan-shaded region (e.g., Gawiser et al. 2007; Bond et al. 2009). However, it is also clear that not all Lyα emitters (LAEs) are LyC leakers, as noted by the magenta dots that are observed to be LyC non-leakers. We interpret this as that the gas being lifted by the supernova-driven momentum is fragmentary such that obscuration or transparency of the LyC sources are sightline dependent even when the gas cloud as a whole is expelled to a high altitude. We note that, if one includes binary evolution effects, such as mergers produced blue stragglers or stripped hot helium stars, additional O stars will emerge with some delay of order 10 Myr. Each of these two delayed components may mount to about 10% of LyC photons produced by initial starburst (Eldridge et al. 2017). This may be a significant addition of LyC sources. Nevertheless, given the closely spaced red contours in Figure 2, we see that none of our conclusions will be significantly altered, if we use $t_h - t_L = 10$ Myr instead of $t_h - t_L = 5$ Myr.

On the right side, the large gulf region occupying about one half of the plot area, gravity dominates over the combined outward force of supernova-explosion-driven momentum flux and radiation pressure. In this region, no complete lift-up of gas to r_h is possible regardless of the duration of the star formation episode. This region contain the blue shaded region labeled as "$z \sim 1$ SFR < 10 $M_\odot$ yr^{-1}," which is a sample of star-forming dwarf galaxies at $z \sim 1$ with SFR < 10 $M_\odot$ yr^{-1} that do not show significant LyC leakage (Rutkowski et al. 2016). The fact that this region lies in the region of the parameter space that is part of the LAE region and indeed is expected not to have large LyC escape is quite remarkable, because the author was not aware of this data set until after the submission of this article. Also in the large gulf region are the Lyman-break galaxies (LBGs), as indicated by the green-shaded region (Giavalisco 2002), suggesting that LBGs are not likely to be copious LyC leakers. However, recent observations (Steidel et al. 2018) indicate a mean $f_{\rm esc} = 0.09 \pm 0.01$ for a subsample of LBGs. This directly contradicts our conclusions. One possible way of reconciliation is that the observed effective radii of LBGs in UV may be overestimates of the effective radii of the star-forming regions; if the actual radii of star-forming regions are in the range of 300–500 pc, LBGs would be located in the region of LyC leakers. Alternatively, star-forming regions of LBGs may be composed of much more compact sub-regions. While not direct proof, it is intriguing to note that Overzier et al. (2009) found that the three brightest of their sample (30 galaxies) of low-redshift analogs of LBGs at $z = 0.1$–0.3 that they examine in detail indeed have very compact sizes, with effective radii no larger than 70–160 pc. Thus, it would be significant to carry out high-resolution FIR observations, such as by Atacama Large Millimeter/submillimeter Array (ALMA), of LBGs to verify if the total star-forming regions are in fact more compact.

As another example, the star near the bottom right is the location of the Milky Way, which is also inside the LyC non-

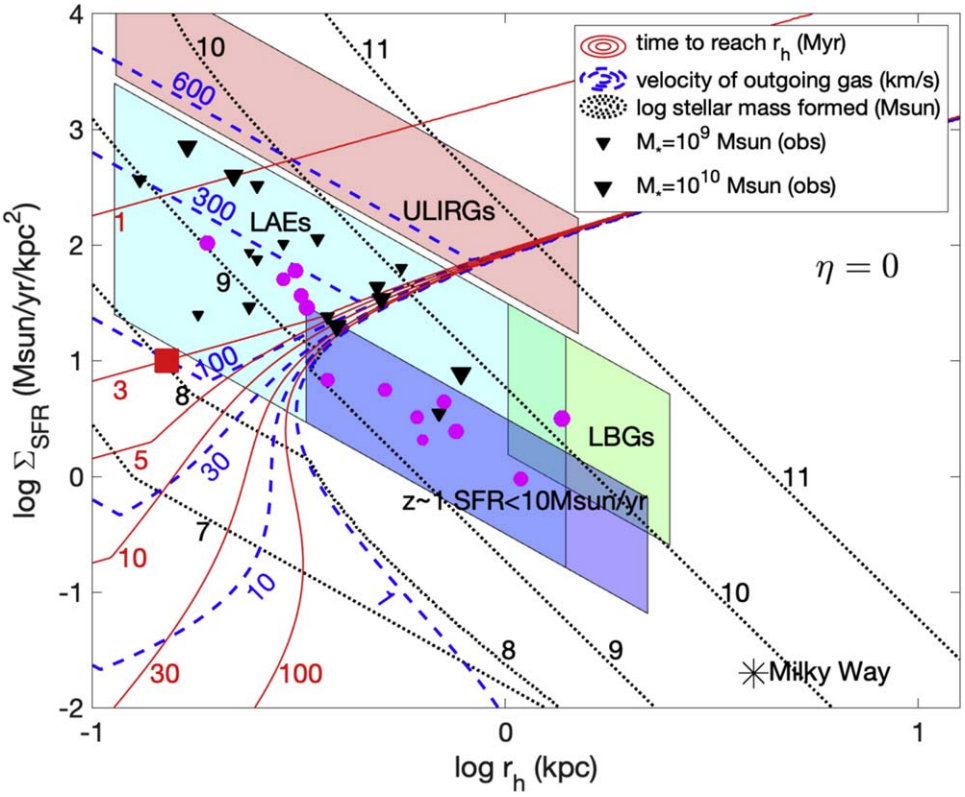

Figure 2. The time that it takes to evacuate the gas to an altitude of r_h, $t_h - t_L$, as the solid red contours labeled in units of Myr, with labels "1," "3," "5," "10," "30," and "100." Shown as dotted black contours are the log of the stellar mass in units of $M_\odot$ formed from this episode, with labels "8," "9," "10," and "11." The dashed blue contours depict the radial velocity of gas being lifted in units of km s^{-1}, with labels "10," "30," "100," "300," and "600." The shaded light blue, light green, light red, and dark blue regions indicate approximately regions normally referred to Lyα emitters (LAEs), Lyman-break galaxies (LBGs) at high redshift, ultra-luminous infrared galaxies (ULIRGs), and $z \sim 1$ star-forming but non-LyC leaking dwarf galaxies, respectively. The LAE region is obtained by using a radius range of 0.1–1.4 kpc and a range of SFR of 1–100 $M_\odot$ yr^{-1} (e.g., Gawiser et al. 2007; Bond et al. 2009). The LBG region is obtained by using a radius range of 1.2–2.5 kpc and a range of SFR of 5–100 $M_\odot$ yr^{-1} (Giavalisco 2002). The ULIRG region is approximately delineated by a radius range of 0.1–1.5 kpc and a range of SFR of 120–1200 $M_\odot$ yr^{-1} (e.g., Spence et al. 2018). The location of the Milky Way galaxy is indicated by a black star near the lower-right corner. The sample of star-forming but non-LyC leaking dwarf galaxies at $z \sim 1$ with SFR < 10 $M_\odot$ yr^{-1} (Rutkowski et al. 2016) is the blue shaded region labeled as "$z \sim 1$ SFR < 10 $M_\odot$ yr^{-1}." Finally, the observed galaxies with large LyC escape fractions are shown as black downward-pointing triangles from various sources (e.g., Alexandroff et al. 2015; Izotov et al. 2016a, 2016b, 2018a, 2018b; Wang et al. 2019), where some galaxies known as LAEs but with little LyC escape are shown as solid magenta dots (Alexandroff et al. 2015). In all cases for M_*, r_h and SFR of observed LyC leakers and non-leakers we use updated values from Wang et al. (2019).

leaker region. Therefore, our Galaxy is unlikely to be a very good LyC leaker for an extragalactic observer. On the other hand, a class of very luminous galaxies—ULIRGs—occupies a region that may straddle the LyC leaker and non-leaker region. ULIRGs are in a special region of the parameter space. It is known that ULIRGs are copious FIR emitters, not known to be LyC leakers. We suggest that ULIRGs may belong to a class of its own, where ram pressure due to gas infall may have helped confine the gas to (1) make them LyC non-leakers and (2) allow for star formation to proceed over a much longer period than indicated by the red contours, despite the strong outward momentum flux driven by ongoing star formation. One way to test this scenario is to search for redshifted 21 cm absorption lines in ULIRGs, if suitable background radio quasars/galaxies or intrinsic central radio quasars/galaxies or possible other bright radio sources.

Nevertheless, we would like to point out that ULIRGs should vary as well. Imagine a merger or other significant event drives an episode of cold gas inflow. The episode spans a period and the starburst triggered goes from the initial phase of build-up when the SFR is extremely subdominant to the inflow gas rate. An estimate of possible gas inflow rates is in order to illustrate the physical plausibility of this scenario. Let us assume that a merger of two galaxies each of halo mass of 10^{12} $M_\odot$ and gas mass 1.6×10^{11} $M_\odot$ triggers a ULIRG event and that 10% of the total gas mass falling onto the central region of size 1 kpc at a velocity of 300 km s^{-1}. Then we obtain a gas infall rate of $\dot{M}_{\rm in} = 1.0 \times 10^4\, M_\odot$ yr^{-1}, which would correspond yield $\eta = (100,\ 10)$ for SFR equal to $(100,\ 1000)\, M_\odot$ yr^{-1}, respectively. In Figure 3 we see that, once the infall rate drops below about 30 times the SFR, gas in ULIRGs would be lifted up by supernovae. This leads to a maximum SFR in ULIRGs that is estimated as follows using this specific merger example. During the build-up phase of the ULIRG, as the gas infall rate exceeds greatly the SFR, one can equate the gas mass to the total dynamical mass. Thus, we have SFR $= c_* M_{\rm gas}[r/(GM_{\rm gas}/r)^{1/2}]^{-1}$. Equating ηSFR (with $\eta = 30$) to $\dot{M}_{\rm in}$, we find the amount of gas accumulated at the maximum gas mass is $M_{\rm gas,max} = 6.3 \times 10^{10}\, M_\odot$, corresponding to a maximum SFR SFR$_{\rm max} = 330\, M_\odot$ yr^{-1} in this case. Thus, our analysis indicates that the physical reason for an apparent maximum SFR in ULIRGs and SMGs may be due to a competition between the maximum ram-pressure confinement of gas and internal supernovae blastwave and radiation pressure. This contrasts with and calls into question the conventional view of radiation pressure alone induced limit on maximum SFR (e.g., Thompson et al. 2005). We defer a more detailed analysis of this subject to a separate paper.

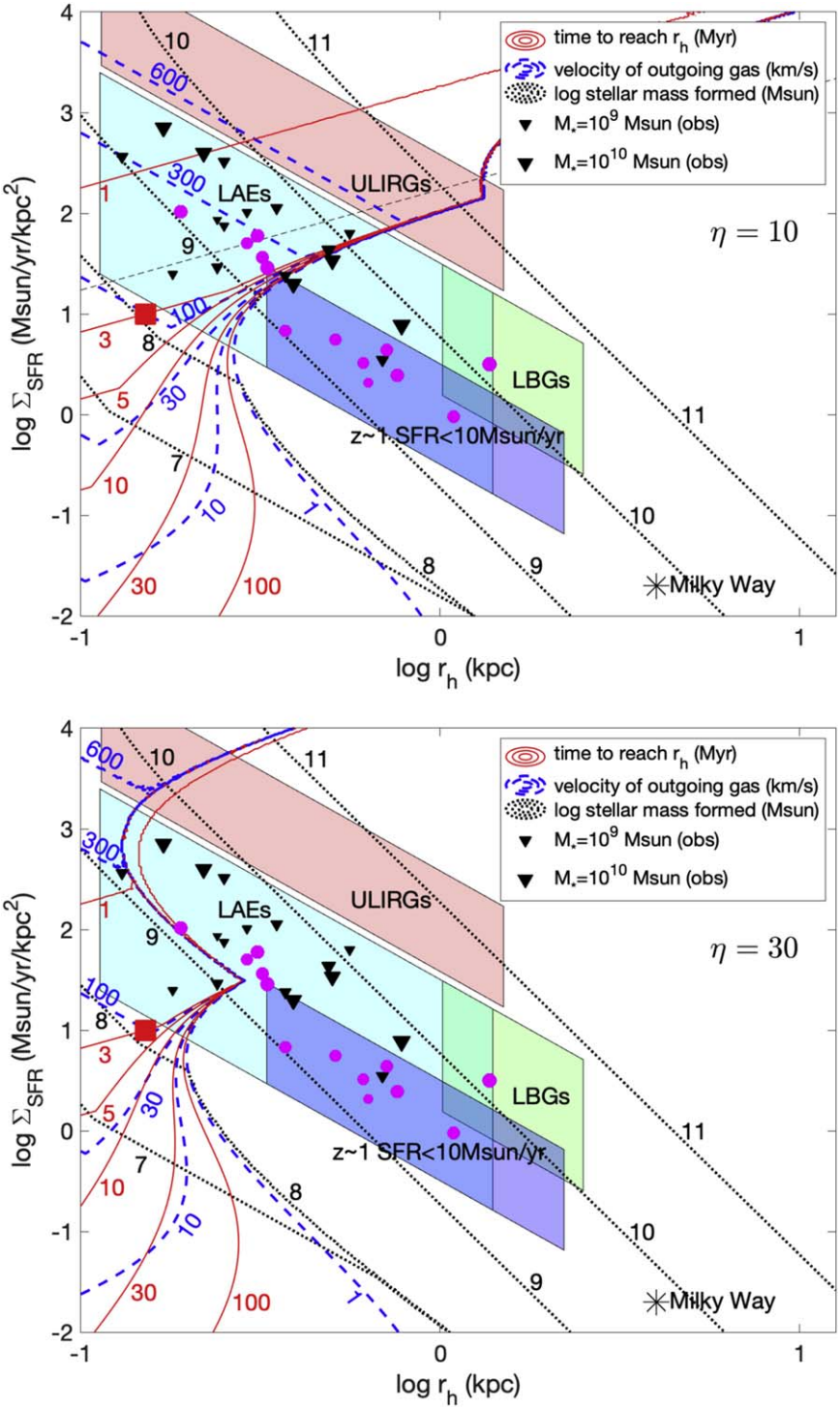

Figure 3. Top panel: similar to Figure 2 with one change: $\eta = 10$ is used here instead of $\eta = 0$ (see Equation (4)) in Figure 2. Bottom panel: similar to the top panel with $\eta = 30$.

At a later point in time it may be transitioned sufficiently rapidly, at least for a subset of ULIRGs, to a phase that is ubiquitous in outflows. Some ULIRGs at this later phase may become significant LyC leakers, if and when the gas inflow rate drops below about 10 times SFR, as shown in Figure 3 by varying the ram pressure (the η parameter, see Equation (4)). This new prediction is in fact consistent with some observational evidence that shows significant Lyα and possibly LyC escape fractions in the advanced stages of ULIRGs (e.g., Martin et al. 2015). These ULIRGs also seem to show blueshifted outflow. It ought to be noted that their measured $f_{\rm esc}$ is relative to the observed far-ultraviolet (FUV) luminosity (i.e., the unobscured region) but not relative to the total SFR, which is difficult to measure. Thus, the escape of LyC in these late stage ULIRGs is a relative statement compared to ULIRGs that are ram pressure confined and are not LyC leakers in the sense that, although in the former the stellar feedback processes may be able to lift gas up, likely still substantial inflow gas may be

able to continue to provide a large amount of obscuring material, albeit less than at earlier phase with a stronger ram-pressure confinement and heavier obscuration.

Let us now turn to the black dotted contours showing the log of the stellar mass in units of $M_\odot$ formed from this episode presumably triggered by a gas accretion event. Two points are worth noting here. First, in the region where LyC leakers are observed, the expected stellar mass formed in a single star formation episode is in the range of 10^8–$10^{10}\,M_\odot$. The observed green-pea galaxies (e.g., Izotov et al. 2016a, 2016b, 2018a, 2018b, 2019; Schaerer et al. 2016) have stellar masses indeed falling in this range. This suggests that a large fraction or all of the stars in green-pea galaxies may be formed in this most recent star formation episode. However, some of the [S II]-weak selected galaxies have stellar masses significantly exceeding $10^{10}\,M_\odot$ (Wang et al. 2019). We suggest that in those cases a large fraction of the stars are formed in previous star formation episodes and spatially more extended than the most recent episode. In both cases—green-pea galaxies and [S II]-weak galaxies—given the central concentration of this most recent star formation episode, it is likely triggered by a low angular momentum gas inflow event. It would be rewarding to searches for signs of such a triggering event, such as nearby companions or post-merger features. Second, there are discontinuities of the contour lines going from the gravity-dominated lower-right region to the outward force dominated upper-left region. This is because, while the gas forms to stars unimpeded in the former, a portion of the gas is blown away in the latter.

Finally, let us turn our attention to the velocity of the gas moving out, as indicated by the blue dashed contours. We see that the outward velocity is in the range of 100–600 $\mathrm{km\,s^{-1}}$. This is a prediction that can be verified by observations when a reasonably large set of data becomes available. Worth noting is that LyC leakers do not necessarily possess outsized outflow velocities. At the present time, the sample of LyC leakers is still relatively small but the approximate range of wind speeds in the range of 150–420 $\mathrm{km\,s^{-1}}$ if one uses directly the separation of Lyα peaks as a proxy (Izotov et al. 2016a, 2016b). We note that given the scattering effects of Lyα photons the separation of Lyα peaks generally may only represent an upper limit on the velocity dispersion, which in turn may be on the same order of the outflow velocity. For a general comparison to young star-forming galaxies without considering LyC escape, Bradshaw et al. (2013) found outflow velocities typically in the range of 0–650 $\mathrm{km\,s^{-1}}$ for young star-forming galaxies with stellar mass of $\sim 10^{9.5}\,M_\odot$, which is consistent with predicted velocity range. Finally, Chisholm et al. (2017) found that LyC leakers (with $f_{\rm esc} \geqslant 5\%$) spans an outflow velocity range of 50–500 $\mathrm{km\,s^{-1}}$ (probed by Si II), consistent with our model. Henry et al. (2015) showed outflow velocities probed by a variety of ions from Si II to Si IV of a range of 50–550 $\mathrm{km\,s^{-1}}$ for green-pea galaxies, consistent with our model once again.

Because the velocity contours are more parallel than perpendicular to the stellar mass contours, a related prediction is that the outflow velocity is expected to be positively correlated with the newly formed stellar mass. Figure 4 shows the median velocity as a function of stellar mass formed in the episode, along with lower and upper quartiles shown as the errorbars, for two cases with $\eta = 0$ and $\eta = 30$. We see clearly a positive correlation between the outflow velocity of LyC leakers and the amount of stars formed in the episode, with median velocity going from $\sim$100 $\mathrm{km\,s^{-1}}$ at $10^8\,M_\odot$ to 600–700 $\mathrm{km\,s^{-1}}$ at $10^{10}\,M_\odot$. For the very high end of the stellar mass of $10^{11}\,M_\odot$ formed in the episode, the outflow velocities are expected to exceed 10^3 $\mathrm{km\,s^{-1}}$. With more data this unique prediction should be testable.

3. Comparisons to Some Previous Works

Heckman & Gas (2001) were among the first to attempt to infer the physical conditions of LyC escape in starburst galaxies combining observational evidence with basic physical considerations in the context of a superbubble driven by supernova explosions. They proposed that strong starbursts clear channels through the neutral ISM to facilitate LyC escape. They ultimately reach the conclusion that the empirical evidence does not demonstrate that galactic winds inevitably produce large values of LyC escape fraction in local starbursts. In other words, galactic outflows appear to be a necessary but not sufficient condition that creates an ISM porous to ionizing radiation. This idea is advanced here in a quantitative fashion. We show that only very compact, high-surface-density starbursting regions are capable of evacuating embedding gas sufficiently and promptly to allow for an environment where a significant amount of LyC escape becomes possible. We argue that this may apply to both a compact starburst at the center of a galaxy or a high-density patch of a spatially extended starburst, because the dynamics are the same in both cases. Nevertheless, we agree with Heckman & Gas (2001) that even in this case the condition created by compact strong starbursts may be a necessary one, due to variations of obscurations along lines of sight, because in most cases gas is only lifted to a limited altitude forming a gas shell that is presumably prone to fragmentation.

In a semi-analytic treatment of escape fraction as a function of star formation surface density, applied to the Eagle simulation, Sharma et al. (2016) adopted a threshold star formation surface density $\Sigma_{\rm SFR} = 0.1\,M_\odot\,\mathrm{yr^{-1}\,kpc^{-2}}$ on a scale of $\sim$1 kpc, motivated by an apparent threshold for driving galactic winds. Our analysis shows that on 1 kpc scale, such a star formation surface density falls short by a factor of 1000 for making conditions to allow for a high LyC escape fraction (see Figure 2). However, when one moves to a smaller size of 0.5 kpc, this threshold star formation surface density lands in the region where gas may be driven away but on a timescale much longer than 5 Myr. In fact, at $\Sigma_{\rm SFR} = 0.1\,M_\odot\,\mathrm{yr^{-1}\,kpc^{-2}}$ there is no parameter space for a high LyC escape fraction, regardless of size. For a star formation surface density $\Sigma_{\rm SFR} = 1\,M_\odot\,\mathrm{yr^{-1}\,kpc^{-2}}$, a region of size $\sim$0.1 kpc can now possess necessary conditions for a high LyC escape fraction. Thus, the overall LyC escape fraction in Eagle simulation they analyze may have been over-estimated. On the other hand, limited numerical resolution may have caused an under-estimation of the star formation surface density in the simulated galaxies there. Thus, the overall net effect is unclear, if all galaxies were resolved and a correct threshold star formation surface density applied. What is likely is that their assessment of the relative contributions of large and small galaxies may have been significantly biased for large ones due to the lenient condition.

Based on an empirical model introduced in Tacchella et al. (2018) that stipulates the SFR to be dependent on halo accretion rate with a redshift-independent star formation efficiency calibrated by N-body simulations, Naidu et al.

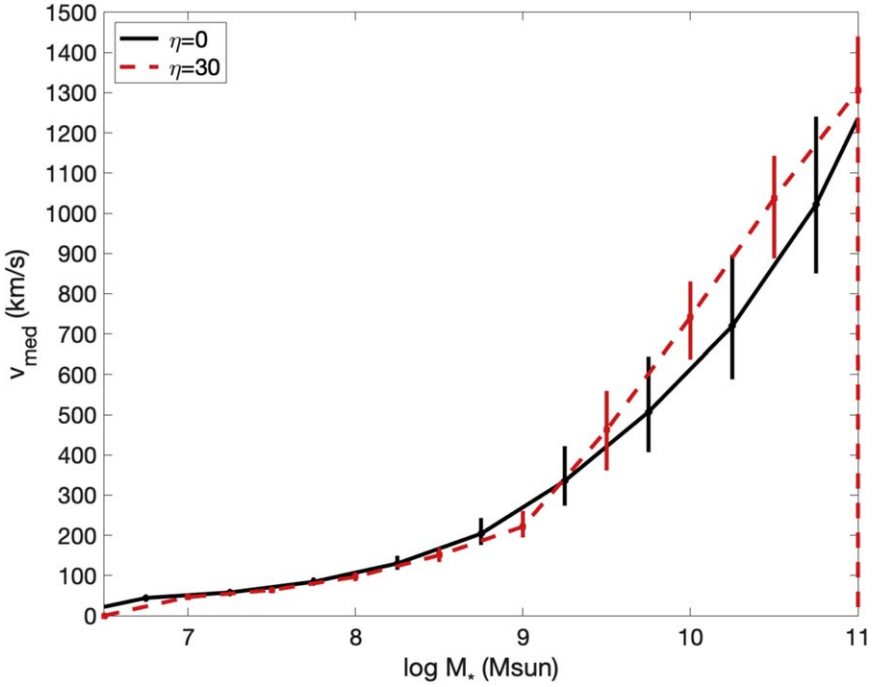

Figure 4. Median velocity as a function of stellar mass formed in the episode, along with lower and upper quartiles shown as the errorbars, for two cases with $\eta = 0$ and $\eta = 30$.

(2019) analyzed how observations of electron scattering optical depth and IGM ionization states may be used to constrain cosmological reionization. Their main assumption is that the LyC escape fraction is constant for all galaxies. Their main conclusion is that bright galaxies ($M_{\rm UV} < -16$) are primarily responsible for producing most of the ionizing photons, in order to produce a rapid reionization process consistent with observations. Our analysis indicates that the assumption of a constant LyC escape fraction for all galaxies may be far from being correct. However, if the bright galaxies are dominated by strong compact central starbursts with high star formation surface densities, an assumed constant LyC escape fraction for all galaxies may lead to a conclusion that faint galaxies make minor contribution to reionization; this conclusion itself ultimately may not be incorrect. It is also worth noting that the galaxy luminosity in their model is substantially shallower than observations below $M_{\rm UV} > -18$. This discrepancy may have, in part, contributed to the more diminished role of faint galaxies in their modeling. These coupled effects suggest an improved, more detailed analysis may be desirable, to better learn the intricate physics.

The dynamics for a central starburst analyzed here in principle is applicable to a compact starbursting subregion within a more extended starbursting disk. The complication in the latter case is that neighboring regions on the disk would unavoidably elevate some gas to varying altitudes, resulting in an environment for the compact starbursting region in question that is subject to more obscuring gas, in lines of sight deviated from the polar direction. Nevertheless, we do expect that the LyC escape is, on average, an increasing function of the star formation surface density within an extended starburst, unless ram pressure becomes a dominant confining process, as likely in the case of most ULIRGs with respect to the SFR surface density.

4. Discussion and Conclusions

A simple analysis of the dynamics of star-forming clouds is performed. The dynamical players include supernova-driven-outward momentum flux, radiation pressure, gravitational force, and ram pressure due to infalling gas. The single most significant finding, evident in Figure 2, is that galaxies able to promptly drive leftover gas away are characterized by two basic properties: small sizes ($\leqslant$1 kpc) and high SFR surface densities ($\Sigma_{\rm SFR} \geqslant 10\,M_\odot\ {\rm yr}^{-1}\,{\rm kpc}^{-2}$). These characteristics are dictated by the twin requirements for removing obscurating material promptly: expelling the gas to a high altitude of the size of the system itself within a few million years since the end of the starburst (which coincides with the onset of the liftoff of the leftover gas from star formation).

As a matter of fact, the only physical commonality among the distinct classes of observed galaxies known to be LyC leakers—green-pea galaxies, [S II]-weak galaxies, some LAEs—are their high SFR surface densities and compact sizes. Our analysis now provides a unifying physical origin for LyC leakers. On the other hand, some other observed properties that differ among different classes are merely symptoms and consequences as a result of gas expulsion, such as those related to density-bound structures and their manifestations due to much reduced gas density around star formation regions in the form of line emission and absorption by a relatively modest amount of gas along the line of sight (O III emission, weak [S II] line, strong Lyα emission, etc.). The compactness of the starburst region likely requires some triggering event to drive the gas to the central region of a new galaxy or an old galaxy rejuvenated. Hence, looking for signs of significant gravitational interactions, such as nearby companions or post-merger features will shed useful light.

In light of this clarification of the physical origin of prodigious LyC leakers, a more robust way to search and identify LyC leakers may be to focus on their basic physical

properties of compactness and high SFR surface density, in addition to likely symptoms as a result of gas expulsion. While such an approach will unite the various disparate kinds of observed LyC leakers physically, it will also help broaden the range of methods that may be employed to search for LyC leakers, which may be important for an adequate account of the overall abundance of LyC leakers. For this undertaking, it is useful to highlight three other verifiable predictions for LyC leakers from this analysis: (1) the newly formed stellar masses are in the range of 10^8–$10^{10}\,M_\odot$, (2) the outflow velocities are in the range typically of 100–600 $\mathrm{km\,s^{-1}}$, (3) a positive correlation between the stellar masses formed and the outflow velocities.

Furthermore, two interesting by-product predictions are also borne out. First, ULIRGs appear to be in a parameter region where they should be prodigious LyC leakers, unless there is a large ram pressure due to infalling gas with a rate exceeding about 30 times the SFR. Then, unavoidably, toward the tail end of a ULIRG event when the ram pressure relents, advanced ULIRGs may turn significant LyC leakers. Second, LBGs with size exceeding 1 kpc are shown not to be prodigious LyC leakers. Thus, if LBGs have significant LyC leakage, as latest observations appear to suggest, it may be that the effective radii of their star-forming regions have been over-estimated by a factor of 2–4.

Finally, an important physical trend is noted. In a hierarchical structure formation model, galaxies at high redshift are, as a whole, more compact and have higher SFR surface densities, simply due to the fact of the universal expansion. In addition, more ubiquitous interactions among galaxies help drive low angular momentum to the central regions of galaxies to facilitate formation of compact systems, on top of already relatively smaller physical sizes of galaxies at high redshift. Therefore, given what is learned in this analysis, it may be predicted that the LyC escape fraction of galaxies is expected to increase with increasing redshift at a given SFR, a given stellar mass, a given luminosity or a given physical size of galaxies. We can also predict that the overall escape fraction for galaxy population as a whole is expected to increase with increasing redshift. This trend helps understand why galaxies at EoR may have much higher escape fractions than their lower-redshift counterparts (e.g., Wise & Cen 2009; Kimm & Cen 2014) and help provide the physical basis for stellar reionization.

We note in passing that simulations that are not able to at least fully resolve star formation regions of size of 100 pc or so may yield results significantly removed from reality, exacerbating plaguing issues, such as overcooling, over-metal enrichment, under-prediction of LyC photon, etc.

I would like to thank the anonymous referee for constructive and helpful comments that significantly improved this paper. I would also like to thank Tim Heckman and Masami Ouchi for discussion, Bengjie Wang, and Tim Heckman for sharing observational data prior to publication, and the warm hospitality of IPMU where this work was initiated. The research is supported in part by NASA grant 80NSSC18K1101.

ORCID iDs

Renyue Cen https://orcid.org/0000-0001-8531-9536

References

Alexandroff, R. M., Heckman, T. M., Borthakur, S., Overzier, R., & Leitherer, C. 2015, ApJ, 810, 104
Bond, N. A., Gawiser, E., Gronwall, C., et al. 2009, ApJ, 705, 639
Bradshaw, E. J., Almaini, O., Hartley, W. G., et al. 2013, MNRAS, 433, 194
Cen, R., & Kimm, T. 2015, ApJL, 801, L25
Chisholm, J., Orlitová, I., Schaerer, D., et al. 2017, A&A, 605, A67
Draine, B. T. 2003, ARA&A, 41, 241
Eldridge, J. J., Stanway, E. R., Xiao, L., et al. 2017, PASA, 34, e058
Fletcher, T. J., Tang, M., Robertson, B. E., et al. 2019, ApJ, 878, 87
Gawiser, E., Francke, H., Lai, K., et al. 2007, ApJ, 671, 278
Giavalisco, M. 2002, ARA&A, 40, 579
Heckman, T. M. 2001, in ASP Conf. Ser. 240, Gas and Galaxy Evolution, ed. J. E. Hibbard, M. Rupen, & J. H. van Gorkom (San Francisco, CA: ASP), 345
Henry, A., Scarlata, C., Martin, C. L., & Erb, D. 2015, ApJ, 809, 19
Izotov, Y. I., Orlitová, I., Schaerer, D., et al. 2016a, Natur, 529, 178
Izotov, Y. I., Schaerer, D., Thuan, T. X., et al. 2016b, MNRAS, 461, 3683
Izotov, Y. I., Schaerer, D., Worseck, G., et al. 2018a, MNRAS, 474, 4514
Izotov, Y. I., Thuan, T. X., & Guseva, N. G. 2019, MNRAS, 483, 5491
Izotov, Y. I., Worseck, G., Schaerer, D., et al. 2018b, MNRAS, 478, 4851
Kimm, T., Blaizot, J., Garel, T., et al. 2019, MNRAS, 486, 2215
Kimm, T., & Cen, R. 2014, ApJ, 788, 121
Krumholz, M. R., Dekel, A., & McKee, C. F. 2012, ApJ, 745, 69
Leitherer, C., Schaerer, D., Goldader, J. D., et al. 1999, ApJS, 123, 3
Lenz, D., Hensley, B. S., & Doré, O. 2017, ApJ, 846, 38
Ma, X., Hopkins, P. F., Kasen, D., et al. 2016, MNRAS, 459, 3614
Martin, C. L., Dijkstra, M., Henry, A., et al. 2015, ApJ, 803, 6
Mostardi, R. E., Shapley, A. E., Steidel, C. C., et al. 2015, ApJ, 810, 107
Naidu, R. P., Tacchella, S., Mason, C. A., et al. 2019, arXiv:1907.13130
Overzier, R. A., Heckman, T. M., Tremonti, C., et al. 2009, ApJ, 706, 203
Rutkowski, M. J., Scarlata, C., Haardt, F., et al. 2016, ApJ, 819, 81
Schaerer, D., Izotov, Y. I., Verhamme, A., et al. 2016, A&A, 591, L8
Shapley, A. E., Steidel, C. C., Strom, A. L., et al. 2016, ApJL, 826, L24
Sharma, M., Theuns, T., Frenk, C., et al. 2016, MNRAS, 458, L94
Spence, R. A. W., Tadhunter, C. N., Rose, M., & Rodríguez Zaurín, J. 2018, MNRAS, 478, 2438
Steidel, C. C., Bogosavljević, M., Shapley, A. E., et al. 2018, ApJ, 869, 123
Tacchella, S., Bose, S., Conroy, C., Eisenstein, D. J., & Johnson, B. D. 2018, ApJ, 868, 92
Thompson, T. A., Quataert, E., & Murray, N. 2005, ApJ, 630, 167
Vanzella, E., de Barros, S., Vasei, K., et al. 2016, ApJ, 825, 41
Verhamme, A., Orlitová, I., Schaerer, D., & Hayes, M. 2015, A&A, 578, A7
Verhamme, A., Orlitová, I., Schaerer, D., et al. 2017, A&A, 597, A13
Wang, B., Heckman, T. M., Leitherer, C., et al. 2019, ApJ, 885, 57
Wise, J. H., & Cen, R. 2009, ApJ, 693, 984
Zapartas, E., de Mink, S. E., Izzard, R. G., et al. 2017, A&A, 601, A29